Identification, Characterization and Site-Saturation Mutagenesis of a Thermostable ω-Transaminase From Chloroflexi Bacterium

Chen Wang
Nanjing Tech University
Kexin Tang
Nanjing Tech University
Ya Dai
Nanjing Tech University
Honghua Jia (hhjia@njtech.edu.cn)
Nanjing Tech University https://orcid.org/0000-0002-3824-7768
Yan Li
Nanjing Tech University
Zhen Gao
Nanjing Tech University
Bin Wu
Nanjing Tech University

Research

Keywords: ω-Transaminase,Chloroflexibacterium, Characterization,Substrate specificity, Site-saturationmutagenesis

Posted Date: March 17th, 2021

DOI: https://doi.org/10.21203/rs.3.rs-296936/v1

Identification, characterization and site-saturation mutagenesis of a thermostable ω-transaminase from *Chloroflexi bacterium*

Chen Wang, Kexin Tang, Ya Dai, Honghua Jia*, Yan Li*, Zhen Gao, Bin Wu

College of Biotechnology and Pharmaceutical Engineering, Nanjing Tech University, Nanjing 211816, China

Correspondent authors: hhjia@njtech.edu.cn; liyan@njtech.edu.cn

Abstract

In present study, we have mined a ω-transaminase (ω-TA) from *Chloroflexi bacterium* from genome database by using an ω-TA sequence ATA117 Arrmut11 from *Arthrobacter* sp. KNK168 and an amine transaminase from *Aspergillus terreus* as templates in a BLASTP search and motif sequence alignment. The protein sequence of the ω-TA from *C. bacterium* shows 38% sequence identity to ATA117 Arrmut11. The gene sequence of the ω-TA was inserted into pRSF-Duet1 and functionally expressed in *E. coli* BL21(DE3). Results showed that the recombinant ω-TA has a specific activity of 1.19 U/mg at pH 8.5, 40 °C. The substrate acceptability test showed that ω-TA has significant reactivity to aromatic amino donors and amino receptors. More importantly, the ω-TA also exhibited a good affinity towards some cyclic substrates such as 1-Boc-3-piperidone. The homology model of the ω-TA was built by Discovery Studio and docking was performed to describe the relative activity towards some substrates. The ω-TA was evolved by site-saturation mutagenesis and found that the Q192G mutant increased the activity to the (R)-α-methylbenzylamine (MBA) by around seven-fold. The Q192G mutant was then used to convert two cyclic ketones, *N*-Boc-3-pyrrolidinone and *N*-Boc-3-aminopiperidine, and the conversions were both improved compared to the parental ω-TA.

Graphical Abstract

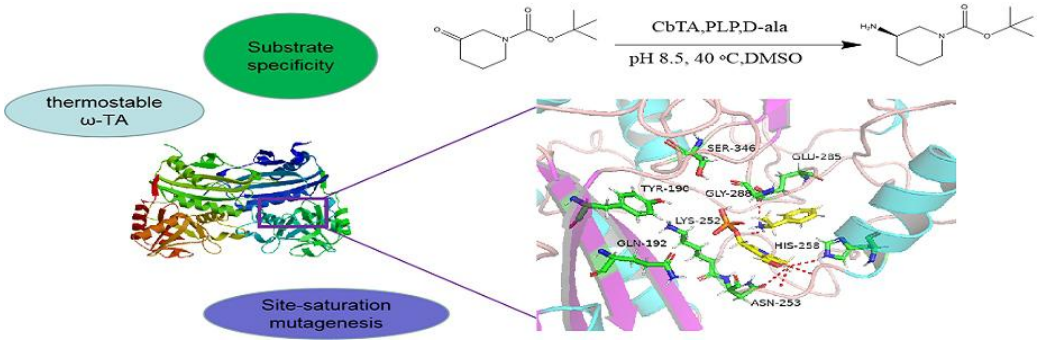

Keywords: ω-Transaminase; *Chloroflexi bacterium*; Characterization; Substrate specificity; Site-saturation mutagenesis

1 Introduction

Chiral amines are very important intermediates, which have a wide range of applications in medicine and fine chemical industries [1]. The production of chiral amines include chemical and biochemical methods. As far as chemical methods are concerned, chiral amines are usually produced by asymmetric catalysis of prochiral molecules, such as hydrogenation of imine or enamine, alkylation of imine, amino hydroxylation and reductive amination [2]. In order to overcome the drawbacks of low enantioselectivity, use of noble metal catalyst, harsh reaction condition, and environmental concern in asymmetric synthesis, several biochemical methods using efficient biocatalysts have been developed, and manage to replace chemical methods. These methods mainly involve enzymes such as amine oxidases, ammonia lyases, amine dehydrogenase and transaminases [3-5]. Among them, ω-transaminases (ω-TAs), which catalyze the transfer of ketone and amino groups, have received extensive attention [6-9]. The well-known example of the synthesis of chiral amines by ω-TAs is the manufacture of sitagliptin, an oral antihyperglycemic drug [10].

Interestingly, ω-TAs originating from various sources have showed distinct selectivity, that is (R)-selective or (S)-selective. Hence, both enantiomers of specific amines can be produced by ω-TAs with different enantioselectivity. Although the ω-TA Ata-117 Arrmut11 from *Arthrobacter* sp. KNK168 is commercially available now, only a few (R)-selective ω-TAs have been identified [11,12]. Therefore, the discovery of novel *R*-selective ω-TAs was still the focus issue in the past few years. Bornscheuer et al. [13,14] developed a method for predicting and screening enzyme function on the basis of key motif in sequence, which has been proved to be effective and successfully used to search and identify 17 (R)-selective ω-TAs by database mining. The method has also been applied to discover five other different sources of (R)-selective ω-TAs [15]. In recent years, more and more (R)-selective ω-TAs have been discerned and investigated, but their wide applications are still limited by the poor properties [16-18]. In order to improve the performance of enzymes, protein engineering has usually been adopted to conduct enzyme design and optimization. A (R)-selective ω-TA has been created by bioinformatic analysis combined with

computational redesign of the D-amino acid aminotransferase, exhibiting a specific activity close to those of natural (R)-selective ω-TAs [19].On the basis of a fluorescence-based screening system, a KnowVolution campaign has been carried out to optimize a (R)-selective ω-TA from *Mycobacterium vanbaalenii* and the best resulting mutant showed specific activity to acetonaphthone more than 100 times higher than parental enzyme [20]. In another study, a (R)-selective ω-TA from *A. cumminsii* ZJUT212 has been modified using a semi-rational protein design, and a mutant has been screened to produce sitagliptin intermediate on a kilogram scale with >99 % e.e. and approximately 80% conversion [21].

In the current study, BLAST (https://blast.ncbi.nlm.nih.gov/Blast.cgi) was performed against thermophilic bacteria in NCBI to identify a putative ω-TA sequence from *Chloroflexi bacterium* using Ata-117 Arrmut11 from *Arthrobacter* sp. KNK168 and amine transaminase from *Aspergillus terreus* as templates. Subsequently, the putative ω-TA gene was cloned into *E. coli* for expression and its kinetic parameters and substrate spectra were characterized. Thereafter, the ω-TA was improved by site-saturation mutagenesis on the basis of reported results and modeling analysis.

2 Materials and Methods

2.1 Reagents

All the chemicals used were of analytical grade and purchased from Shanghai Aladdin Biochemical Technology Co., Ltd. or Sigma-Aldrich, Inc. unless otherwise noted.

2.2 Sequence analysis

The Ata-117 Arrmut11 sequence from *Arthrobacter* sp. KNK168 and amine transaminase from *A. terreus*, were used as templates for BLAST search in NCBI to find new ω-TA sequence. After removing incomplete and redundant sequences, MEGA 7.0 was used to align all unknown sequences, and the target sequences which conform to the functional characteristics of (R)-selective ω-TA were screened out according to the motif sequence confirmed in reference [9]. Among them, a putative (R)-selective ω-TA from *C. bacterium* was chosen for further study, which shows 38% identity with Ata-117 Arrmut11. A phylogenetic tree was also generated with MEGA 7.0 [22] by using the neighbor-joining algorithm [23].

2.3 Plasmid and strain Construction

The gene sequence of the putative (R)-selective ω-TA from *C. bacterium* was further

codon-optimized and synthesized by GenScript (Nanjing, China). The encoding region was inserted between the BamH I and Xho I, with a 6-histidine tag at the *N*-terminal, resulting in plasmid pRSF-*CbTA*. The recombinant plasmid was transformed into *E. coli* BL21(DE3) to generate the recombinant strain of *E. coli* BL21(DE3)/pRSF-*CbTA*.

2.4 Expression and purification of recombinant ω-TA

The recombinant *E. coli* BL21(DE3)/pRSF-*CbTA* was cultured in 100 mL LB medium (1.0% peptone, 0.5% yeast extract, and 1.0% NaCl) with kanamycin (50 μg/mL) at 37 °C and 200 rpm. When the OD_{600} of the culture reaches about 0.6, 0.02 mM isopropyl β-D-1-thiogalactopyranoside (IPTG) was added, and the culture was cultivated at 20 °C for another 24 h. Thereafter the cells were harvested and re-suspended in 20 mL of glycine-NaOH buffer (50 mM, pH 8.5), and sonicated in an ice bath for 30 min. The cell debris was removed by centrifugation at 8000 × g at 4 °C for 40 min. The supernatant was passed through a 5 mL Ni-NTA column to purify the recombinant ω-TA, and then the purified ω-TA solution was then stored at 4 °C for further experiments. The molecular weight of the purified ω-TA were determined by 12% (w/v) SDS-PAGE [24]. A control experiment was performed under the same conditions using *E. coli* transformant carrying empty pRSFDuet-1.

2.5 Assay of enzyme activity

Enzyme activity analysis was performed in 500 μL glycine-NaOH buffer (50 mM, pH 8.5) containing pyridoxal 5'-phosphate (PLP) (20 μM), (R)-α-methylbenzylamine (MBA, 10 mM), sodium pyruvate (10 mM). The reaction started at 40 °C by adding 0.05 mg of the purified ω-TA to the mixture. After 30 min the mixture was heated and boiled for 20 min to stop the reaction. All experiments were performed in three replicates. The resulting acetophenone was analyzed by HPLC. One unit of enzyme activity is defined as the amount of ω-TA catalyzing the release of 1 μmol acetophenone per minute.

2.6 HPLC analysis

The acetophenone was measured at 254 nm by HPLC (Agilent 1260) using an Agilent C18 column (250 mm × 4.6 mm) at 30 °C [25]. The mobile phase is water/acetonitrile (50/50, v/v) and the flow rate is 1 mL/min.

The chiral MBA were detected by HPLC (Agilent 1260) with a CR-I(+) chiral column (150 mm × 3.0 mm) (Daicel Corp.) at 254 nm and 30 °C. The eluent is water/acetonitrile (70/30, v/v)

containing 0.36% trifluoroacetic acid at a flow rate of 0.4 mL/min.

The analyses of *N*-Boc-3-pyrrolidinone and *N*-Boc-3-aminopyrrolidine were performed on a HPLC system (Agilent 1260) with an Agilent C18 column (250 mm × 4.6 mm) at 220 nm and 25 °C. Elution was carried out with mobile phase of water/acetonitrile/diethanolamine (70/30/0.1, v/v/v) at a rate of 1 mL/min[26].

2.7 Characterization of biochemical properties

By using the following buffers with different pH 6.0-10.5 (50 mM phosphate buffer, pH 6.0-8.0; 50 mM glycine-NaOH buffer, pH 8.5-10.5), the optimal pH of the ω-TA was determined at 40 °C. The optimal temperature for the ω-TA was investigated from 25 °C to 65 °C at pH 8.5. Relative activity (%) was calculated using the maximal activity as a control (100%). The temperature stability was measured by incubating the ω-TA for a period in the temperature range of 40-65 °C .

The tolerance of the ω-TA to organic solvents is determined by incubating 100 μL of the ω-TA in glycine-NaOH buffer (50 mM, pH 8.5) for 5 h at room temperature. The buffer contains 0%, 5%, 10%, 20%, 40%, 60%, 80% (v/v) organic co-solvents (acetonitrile or DMSO or methanol or ethanol). After that, residual activities were evaluated using the assay method of enzyme activity described above.

2.8 Determination of kinetic parameters

The kinetic parameters of the ω-TA to (R)-MBA or pyruvate were measured at 45 °C and pH 8.5. According to the method described above, the initial reaction rate was determined under the conditions of different concentrations of (R)-MBA or pyruvate. The production of acetophenone and the consumption of pyruvate were analyzed by HPLC. In order to determine the kinetic parameters of the ω-TA to (R)-MBA, the reaction solution was 500 μL glycine-NaOH buffer (50 mM, pH 8.5) containing 20 mM pyruvate, 0.05 mg ω-TA, 0.02 mM PLP, and different concentrations of (R)-MBA. The kinetic parameters of the ω-TA to pyruvate was measured in 500 μL glycine-NaOH buffer (50 mM, pH 8.5) containing 20 mM (R)-MBA, 0.05 mg of ω-TA, 0.02 mM PLP, and different concentrations of sodium pyruvate. The K_m and k_{cat} values of (R)-MBA and pyruvate were calculated according to the nonlinear regression fitting of Michaelis-Menten equation.

2.9 Characterization of the substrate specificity of the ω-TA

Substrate specificity of the ω-TA was tested by reaction between different groups of amino donors

and amino receptors. All experiments were performed in triplicate. When the specificity of the amino donors were studied, the amino donors were listed in table 2,3. The activity assay for each reaction was carried out in a 50 mM glycine-NaOH buffer (pH 8.5) containing 25 mM amino donor, 25 mM sodium pyruvate, 0.02 mM PLP and a suitable amount of purified enzyme, with a final volume of 500 μL at 40 °C for 30 min. When the specificity of the amino receptors were studied, the amino receptors were listed in table 4,5. The activity assay for each reaction was carried out in a 50 mM glycine-NaOH buffer (pH 8.5) containing 25 mM (R)-MBA, 25 mM amino receptors, 0.02 mM PLP and a suitable amount of purified enzyme, with a final volume of 500 μL at 40 °C for 30 min

2.10 Molecular modeling and substrate docking

Molecular modeling was performed using Modeller 9.24 and I-Tasser (https://zhanglab.ccmb.med.umich.edu/I-Tasser/). The homology model was based on the crystal structure (PDB: 3WWH, 4CE5, 4CMD, 4UUG, 5E25), and the best model was selected by Ramachandran analysis.

2.11 Site-saturation mutagenesis

The amino acid residues Y190, Q192, and G288 were selected for site-saturation mutagenesis on the basis of previous results and modeling analysis [19]. The site saturation mutagenesis was designed by NDT codon design. All primers are listed in Table 1. Site saturation mutagenesis was performed according to the instructions of the site-directed mutagenesis kit (MutExpress II Fast Mutagenesis Kit V2, Vazyme, Nanjing, China). Mutations were introduced by mutagenesis polymerase chain reaction (PCR). The amplified fragments were digested with DpnI at 37 °C for 1 h and the recombinant plasmid was transformed into *E. coli* BL21(DE3) for screening. Individual colonies of the transformants were transferred to 96-well plates containing 300 μL of LB medium with kanamycin (50 μg/mL), 96-well plate were incubated overnight (37 °C, 200 rpm). Subsequently, 30 μL of that culture suspension was transferred to a medium containing 300 μL of fresh LB in each well for culture for 2 h (37 °C , 200 rpm), and then 300 μL of LB containing 0.04 mM IPTG was added and induced at 20 °C for 24 h and the sludge was collected by centrifugation at 4200 rpm for 20 min. The cells were fragmented according to the fragmentation kit (xTractorTM Buffer Kit, TAKARA, Japan). After the cells were allowed to stand at room

temperature for 30 min, the crude mutant ω-TA solution was collected by centrifugation. Thereafter, the activity of the mutant was tested as described above.

Table 1 List of primer sequences for the creation of the ω-TA variants

Primer name	5’ → 3’ nucleotide sequence
Y190R F	GAT GCG CGT GTT CAG GTG ATC GTT ACC CGT
Y190R R	CTG AAC ACG CGC ATC ACG GTG ACC CGC ACG
Y190P F	GAT GCG TTT GTT CAG GTG ATC GTT ACC CGT
Y190P R	CTG AAC AAA CGC ATC ACG GTG ACC CGC ACG
Y190L F	GAT GCG CTT GTT CAG GTG ATC GTT ACC CGT
Y190L R	CTG AAC AAG CGC ATC ACG GTG ACC CGC ACG
Y190I F	GAT GCG ATT GTT CAG GTG ATC GTT ACC CGT
Y190I R	CTG AAC AAT CGC ATC ACG GTG ACC CGC ACG
Y190V F	GAT GCG GTT GTT CAG GTG ATC GTT ACC CGT
Y190V R	CTG AAC AAC CGC ATC ACG GTG ACC CGC ACG
Y190S F	GAT GCG AGT GTT CAG GTG ATC GTT ACC CGT
Y190S R	CTG AAC ACT CGC ATC ACG GTG ACC CGC ACG
Y190H F	GAT GCG CAT GTT CAG GTG ATC GTT ACC CGT
Y190H R	CTG AAC ATG CGC ATC ACG GTG ACC CGC ACG
Y190N F	GAT GCG AAT GTT CAG GTG ATC GTT ACC CGT
Y190N R	CTG AAC ATT CGC ATC ACG GTG ACC CGC ACG
Y190A F	GAT GCG GAT GTT CAG GTG ATC GTT ACC CGT
Y190A R	CTG AAC ATC CGC ATC ACG GTG ACC CGC ACG
Y190C F	GAT GCG TGT GTT CAG GTG ATC GTT ACC CGT
Y190C R	CTG AAC ACA CGC ATC ACG GTG ACC CGC ACG
Y190G F	GAT GCG GGT GTT CAG GTG ATC GTT ACC CGT
Y190G R	CTG AAC ACC CGC ATC ACG GTG ACC CGC ACG
Q192R F	TAC GTT CGT GTG ATC GTT ACC CGT GGT CTG
Q192R R	GAT CAC ACG AAC GTA CGC ATC ACG GTG ACC
Q192P F	TAC GTT TTT GTG ATC GTT ACC CGT GGT CTG

Q192P R	GAT CAC AAA AAC GTA CGC ATC ACG GTG ACC
Q192L F	TAC GTT CTT GTG ATC GTT ACC CGT GGT CTG
Q192L R	GAT CAC AAG AAC GTA CGC ATC ACG GTG ACC
Q192I F	TAC GTT ATT GTG ATC GTT ACC CGT GGT CTG
Q192I R	GAT CAC AAT AAC GTA CGC ATC ACG GTG ACC
Q192V F	TAC GTT GTT GTG ATC GTT ACC CGT GGT CTG
Q192V R	GAT CAC AAC AAC GTA CGC ATC ACG GTG ACC
Q192S F	TAC GTT AGT GTG ATC GTT ACC CGT GGT CTG
Q192S R	GAT CAC ACT AAC GTA CGC ATC ACG GTG ACC
Q192Y F	TAC GTT TAT GTG ATC GTT ACC CGT GGT CTG
Q192Y R	GAT CAC ATA AAC GTA CGC ATC ACG GTG ACC
Q192H F	TAC GTT CAT GTG ATC GTT ACC CGT GGT CTG
Q192H R	GAT CAC ATG AAC GTA CGC ATC ACG GTG ACC
Q192N F	TAC GTT AAT GTG ATC GTT ACC CGT GGT CTG
Q192N R	GAT CAC ATT AAC GTA CGC ATC ACG GTG ACC
Q192A F	TAC GTT GAT GTG ATC GTT ACC CGT GGT CTG
Q192A R	GAT CAC ATC AAC GTA CGC ATC ACG GTG ACC
Q192C F	TAC GTT TGT GTG ATC GTT ACC CGT GGT CTG
Q192C R	GAT CAC ACA AAC GTA CGC ATC ACG GTG ACC
Q192G F	TAC GTT GGT GTG ATC GTT ACC CGT GGT CTG
Q192G R	GAT CAC ACC AAC GTA CGC ATC ACG GTG ACC
G288R F	AGC CGT CGT GCG AAC GTG TTT CTG ATT CAA
G288R R	GTT CGC ACG ACG GCT TTC GGT CAG GTA ACC
G288P F	AGC CGT TTT GCG AAC GTG TTT CTG ATT CAA
G288P R	GTT CGC AAA ACG GCT TTC GGT CAG GTA ACC
G288L F	AGC CGT CTT GCG AAC GTG TTT CTG ATT CAA
G288L R	GTT CGC AAG ACG GCT TTC GGT CAG GTA ACC
G288I F	AGC CGT ATT GCG AAC GTG TTT CTG ATT CAA
G288I R	GTT CGC AAT ACG GCT TTC GGT CAG GTA ACC

G288V F	AGC CGT GTT GCG AAC GTG TTT CTG ATT CAA
G288V R	GTT CGC AAC ACG GCT TTC GGT CAG GTA ACC
G288S F	AGC CGT AGT GCG AAC GTG TTT CTG ATT CAA
G288S R	GTT CGC ACT ACG GCT TTC GGT CAG GTA ACC
G288Y F	AGC CGT TAT GCG AAC GTG TTT CTG ATT CAA
G288Y R	GTT CGC ATA ACG GCT TTC GGT CAG GTA ACC
G288H F	AGC CGT CAT GCG AAC GTG TTT CTG ATT CAA
G288H R	GTT CGC ATG ACG GCT TTC GGT CAG GTA ACC
G288N F	AGC CGT AAT GCG AAC GTG TTT CTG ATT CAA
G288N R	GTT CGC ATT ACG GCT TTC GGT CAG GTA ACC
G288A F	AGC CGT GAT GCG AAC GTG TTT CTG ATT CAA
G288A R	GTT CGC ATC ACG GCT TTC GGT CAG GTA ACC
G288C F	AGC CGT TGT GCG AAC GTG TTT CTG ATT CAA
G288C R	GTT CGC ACA ACG GCT TTC GGT CAG GTA ACC

3 Results and discussion

3.1 Sequence analysis

Nowadays, more and more protein sequences are stored in the database, which provides a huge resource for the mining of biocatalysts. Two independent BLAST searches were performed using two crystallized (R)-selective ω-TAs, Ata-117 Arrmut11 (PDB: 5FR9) from *Arthrobacter* sp. KNK168 and amine transaminase (PDB: 4CE5) from *A. terreus* as templates. Then a rational analysis of the aligned sequences was performed use motif sequence alignment following the criteria previously established by Höhne and coworkers [13]. Four putative sequences derived from thermophilic bacteria were obtained from the NCBI non-redundant protein sequence library. According to preliminary activity test, the ω-TA from *C.* bacterium with the highest activity was selected as the target.

The ω-TA from *C. bacterium* showed identity with amine transaminases from the following microorganisms: *Arthrobacter* sp. KNK168 (PDB: 3WWH; 38%), *A. fumigatus* Af293 (GenBank accession No. EAL86783; 37.2%), *Archaeoglobus fulgidus* DSM 4304 (PDB: 5MQZ; 37.8%), *Nectria haematococca* MPVI (PDB: 4CMD; 36.8%), *M. vanbaalenii* PYR-1 (GenBank accession

No. ABM15291; 35.9%) and *Geoglobus acetivorans* (PDB: 5e25; 35.8%). Phylogenetic tree analysis was performed to verify the taxonomic and evolutionary relationship of the ω-TA to previously reported transaminases, and the results are presented in Fig. 1. Ten amino acid sequences with different degrees of sequence identity to the ω-TA were collected and compared. The ω-TA was found to have a close evolutionary relationship with other sequences, except for thermophilic archaea *G. acetivoras.*

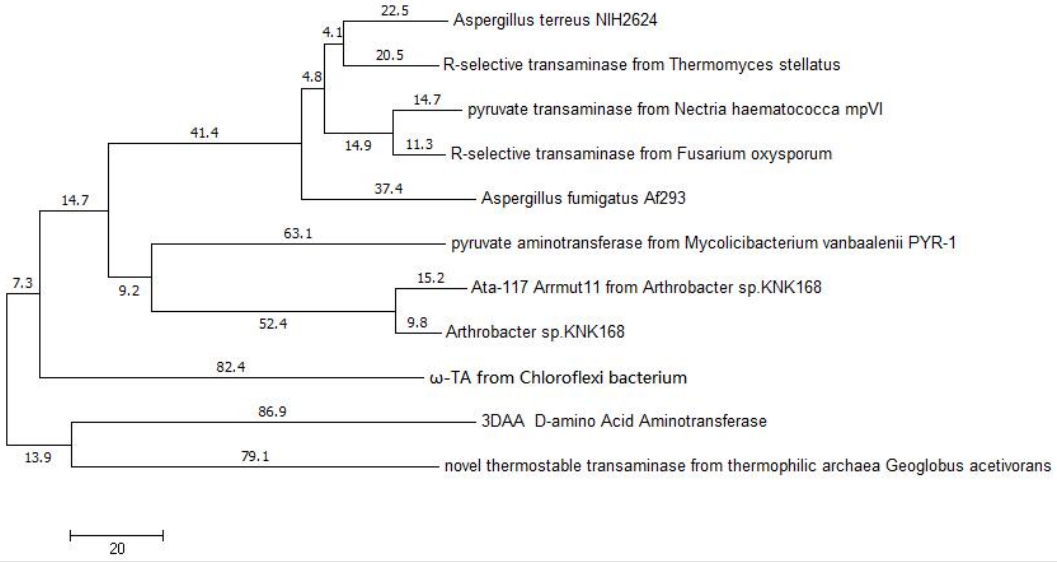

Fig. 1 Phylogenetic analysis of the ω-TA from *C. bacterium* and related proteins. The phylogenetic tree was constructed using the neighbor-joining algorithm in the molecular evolutionary genetics analysis package (MEGA 7) and highlighted the relative positions of the proteins labeled with the species names.

3.2 Purification and identification of recombinant ω-TA

The recombinant *E. coli* BL21(DE3)/pRSF-*CbTA* cells were cultured, collected and sonicated. The expressed recombinant protein with a theoretical molecular weight of 44.3kda accounted for more than 30% of the total protein in the cells, and was detectable in both the soluble and insoluble parts of *E. coli* BL21 (DE3)/pRSF-*CbTA* cells (Fig. 2). The recombinant protein was purified by immobilized metal ion affinity chromatography with the assistance of His-tag at the *N*-terminus of the sequence, and the purification results are shown in Fig. 2. The followed activity test indicated that the specific activity of the ω-TA was 1.19U/mg at pH 8.5, 40 °C.

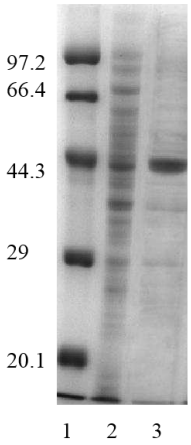

Fig. 2 SDS-PAGE of the ω-TA. Lane 1, protein markers; Lane 2, crude extract; Lane 3, purified enzyme

3.3 Enzymatic properties of the ω-TA

As is showed in Fig. 3a, the effect of pH on the ω-TA activity was assessed over the range of pH 6.0 to 10.5, and the ω-TA has the highest activity at pH 8.5, which is similar to the known ω-TAs [27, 28]. For example, a typical (R)-selective ω-TA *Arthrobacter* sp. KNK168 has showed an optimal pH of 8.0 to 9.0 [29]. Besides, a branched-chain amino acid aminotransferase TUZN1299 identified from the genome of the hyperthermophilic archaeon *Thermoproteus uzoniensis* has exhibited the optimal pH of 8.0 [30]. The effect of temperature on the ω-TA activity was evaluated over the range of 25–65 °C, and the highest activity was detected at 45 °C (Fig. 3b). Fig. 3c presents the temperature profile of the ω-TA, and results the ω-TA has good thermal stability. Interestingly, with the increase of incubation time at 45 °C, the highest activity of the ω-TA can reach twice of the original activity, which was similar to an (S)-selective thermophilic transaminase from *Geobacillus thermodelinificans* [31]. This increase in activity may be due to the elevated stable interaction of temperature dependent folding [32]. The temperature dependence also showed that the ω-TA remain more than 50% activity after 12 h of incubation at 50–55 °C, but the ω-TA was significantly inactivated at above 60 °C. Similarly, most of the thermophilic TAs have showed significant thermal stability at about 55 °C [33]. For instance, it has been found that a transaminase identified from *Thermomicrobium roseum* retained 50% activity after 5 h of incubation at 70 °C [34]. A β-amino acid transaminase Ms-TA2 has also been discovered from a *Meiothermus* strain isolated in an Icelandic hot spring, which kept around 60% activity after incubation at 50 °C for 3 h [35]. However, few thermophilic TAs remain active after incubation at

temperatures above 65 °C. A novel amine transaminase has demonstrated spectacular thermostability, and it activity can be maintained at 85% or around 40% after being incubated at 80 °C for 5 d or 14 d [36].

Organic cosolvent is very necessary to increase the solubility of substrates. The influence of organic cosolvent on the ω-TA activity was determined by adding methanol, ethanol, DMSO and acetonitrile in reaction solutions (Fig. 3d). Results showed that the ω-TA activity increased significantly in all four 20-40% organic co-solvents, while decreased in 60% organic co-solvents. This indicates that ω-TA is well tolerated by organic solvents and the results are superior to that of a solvent-tolerant haloarchaeal (R)-selective transaminase isolated from a Triassic Period salt mine [37].

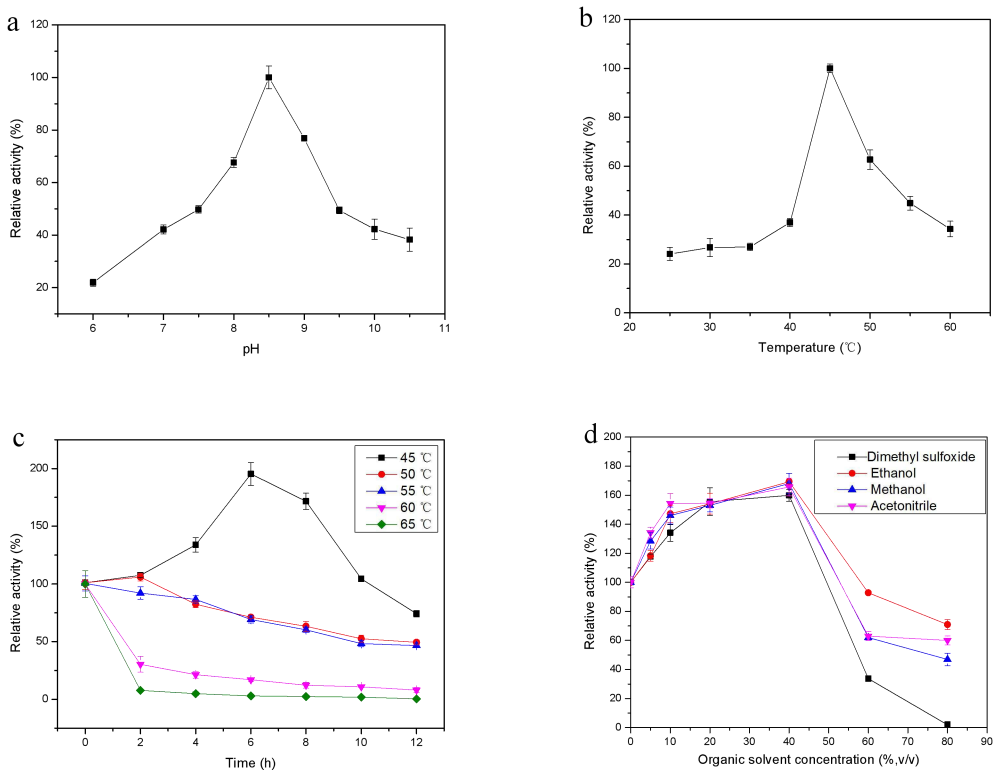

Fig. 3 Characterization of enzymatic properties of the ω-TA. **a)** Optimum pH; **b)** Optimum temperature; **c)** Temperature stability; **d)** Effect of Organic cosolvent concentration on the ω-TA activity.

3.4 Kinetic Parameters of the ω-TA

The kinetic parameters are helpful to evaluate the catalytic ability of enzymes. Given that transaminases operate via a typical dual substrate recognition, the K_m and k_{cat} to either substrate of

the ω-TA were determined by changing the concentration of (R)-MBA or pyruvate from 2.5 mM to 40 mM respectively. With 20 mM pyruvate as co-substrate, the K_m and k_{cat} of the ω-TA to (R)-MBA are 14.68 mM and 3397.63 s^{-1}, while the K_m and k_{cat} of the ω-TA for pyruvate are 2.834 mM and 1617.5 s^{-1}, respectively. Compared with the ATA117 from *Arthrobacter* sp. KNK168, the ω-TA showed similar affinity for pyruvate, but its K_m value for (R)-MBA was significantly higher than that of ATA117, which indicated that the ω-TA had slightly lower affinity for amine. However, the ω-TA showed lower K_m to pyruvate and higher k_{cat} than a transaminase from *Fusarium oxysporum* [38], which means higher reactivity on pyruvate (Fig. 4).

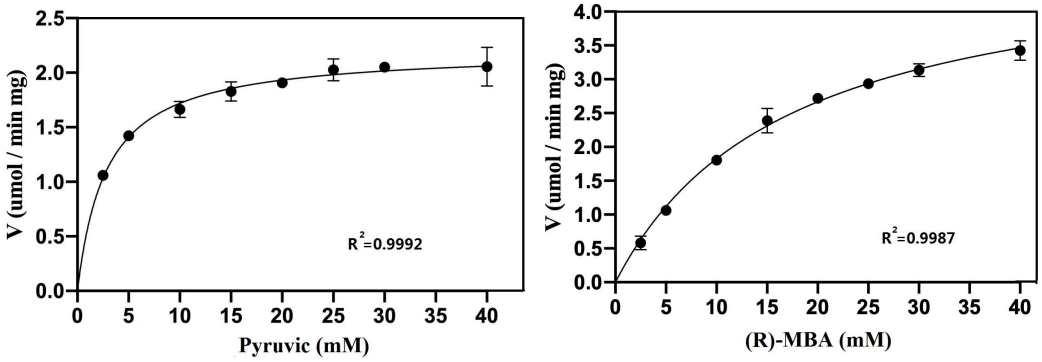

Fig. 4 The nonlinear regression fitting of Michaelis-Menten equation

3.5 Substrate specificity of the ω-TA

Previous studies on substrate range and stereoselectivity have shown that the active center of transaminase is composed of two active pockets. The large pocket can embrace the large structure and the small pocket is usually limited to methyl-sized substituents [39]. Considering the binding of the substrate to the ω-TA active center, we resolved the structure of the substrate on the basis of the ω-TA active site model, ω-TA's large pocket uses R1, while ω-TA's small pocket contains R2. All substrates were divided into four groups: aromatic and aliphatic amines, amino acids, ketones and aldehydes to allow us to compare reactivity chemically.

Table 2 Amino donor specificity of the ω-TA for aliphatic and aromatic amines

Amino donor	R1	R2	Relative activity (%)[a]
A1	$–C_6H_5$	$–CH_3$	100
A2	$–CH_3CH_2$	–H	66
A3	$–CH_3$	$–CH_3$	＜1

A4	–CH_2CH_3	–CH_3	nd
A5	–$(CH_2)_2(CH_3)_2$	–H	50
A6	–CH_2CH_3	–CH_2CH_3	38
A7	–$(CH_2)_4CH_3$	–CH_3	67
A8	–$(CH_2)_5CH_3$	–CH_3	109
A9	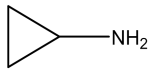		60
A10	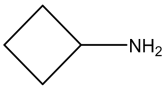		61
A11	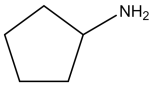		74
A12	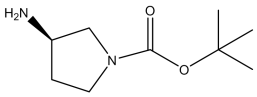		35
A13	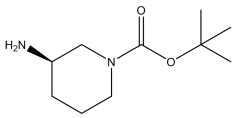		85
A14	–C_6H_5	–H	＜1
A15	-$CH_2C_6H_5$	–H	42
A16	–$CH_2C_6H_5$(4-OH)	–H	76
A17	–C_6H_4(3-Cl)	–CH_3	115
A18	–$(CH_2)_2C_6H_5$	–CH_3	82

Table 3 Amino donor specificity of the ω-TA for amino acids

Amino donor	R1	R2	Relative activity (%)[a]
B1	–$(CH_2)_2COOH$	–COOH	36
B2	–$(CH_2)_3NHNH_2NH$	–COOH	38
B3	–CH_2SH	–COOH	48
B4	–COOH	–CH_3	24.6
B5	–CH_2COOH	–CH_3	4

[a] Reaction conditions in Table 2 and Table 3: 0.1 mg mL^{-1} purified enzyme, 25 mM pyruvate and either 25 mM amino donor, 1 mL glycine-NaOH buffer (50 mM, pH 8.5) and 40 °C. One unit of

the enzyme activity was defined as the conversion of 1 μmol pyruvate per minute. The relative activity for (R)-MBA was designated as 100%.

Table 4 Amino acceptor specificity of the ω-TA for keto acids and ketones

Amino acceptor	R1	R2	Relative activity (%)[b]
C1	–COOH	$–CH_3$	100
C2	$–CH_2CH_3$	$–CH_3$	nd
C3	$–CH_2CH_3$	$–CH_2CH_3$	nd
C4	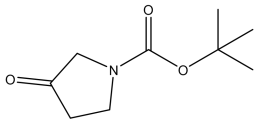		2.4
C5	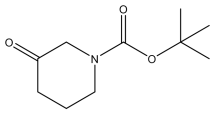		14.7
C6	$–(CH_2)_2COOH$	–COOH	nd
C7	$–C_6H_4(2\text{-}NO_2)$	$–CH_3$	238
C8	$–C_6H_4(4\text{-}OCH_3)$	$–CH_3$	259
C9	$–C_6H_4(2\text{-}OH)$	$–CH_3$	21.8
C10	$–C_6H_4(2\text{-}Br)$	$–CH_3$	＜1
C11	$–C_6H_4(2\text{-}F)$	$–CH_3$	2.9
C12	$–C_6H_4(2\text{-}CH_3)$	$–CH_3$	2.4
C13	$–C_6H_5$	$–CH_2OH$	nd
C14	$–C_6H_5$	$–(CH_2)_3CH_3$	nd
C15	$–CH_2C_6H_5$	$–CH_2C_6H_5$	6

Table 5 Amino acceptor specificity of the ω-TA for aldehydes

Amino acceptor	R1	R2	Relative activity (%)[b]
D1	$–CH_2CH_3$	–H	1.2
D2	$–(CH_2)_2CH_3$	–H	6
D3	$–CH(CH_3)_2$	–H	5.7
D4	$–CH(CH_2)_4(CH_3)_2$	–H	5.8
D5	$–C_6H_5$	–H	272
D6	$–C_6H_3(2\text{-}OH)(5\text{-}NO_2)$	–H	250

D7	$-CH_2C_6H_5$	–H	26

[b] Reaction conditions in Table 4 and Table 5: 0.1 mg mL^{-1} purified enzyme, 25 mM (R)-MBA and either 25 mM amino acceptor, 1 mL glycine-NaOH bufer (50 mM, pH 8.5) and 40 °C. One unit of the enzyme activity was defined as the conversion of 1 μmol acetophenone per minute. The relative activity for pyruvate was designated as 100%.

As is showed in Table 2, Table 3, Table 4 and Table 5, we can find that the ω-TA can utilize a wide range of amino donors and acceptors for the substrate range, which is consistent with the literature [25], indicating their potential for synthetic applications. It can be seen from Table 2 that the ω-TA has good activity for most aliphatic and aromatic amines, but there are a marked difference among various aliphatic or aromatic amines, which is similar to the results reported by Jiang et al[15]. A comparison of the relative activity of the ω-TA to aliphatic amines revealed that it showed higher activity for the long chain amines (A5-A8), while it exhibited a very low reactivity against the short chain amines isopropylamine (A3) and 2-butylamine A4) except for propylamine (A2). Interestingly, the ω-TA displayed higher reactivity to propylamine but extremely low to isopropylamine unlike other amine transaminases. Furthermore, the ω-TA is quite reactive to cyclic amines, and its relative activity is normally better with the increase of the ring (A9-A13). Unexpectedly, when amino acids are used as the amino donors (B1-B4), the activity given by ω-TA is not very high, or even very low, e.g. 2-aminobutyric acid (B5).

The amino receptor specificity of the ω-TA was studied and the results are presented in Table 4 and Table 5. The ω-TA appears to have similar amino receptor specificity for *Capronia semiimmersa* [40]. The amino receptor spectrum shows that nearly all aliphatic, cyclic, and aromatic ketones show low reactivity except for 2'-nitroacetophenone (C7), 4'-methoxyacetophenone (C8), benzaldehyde (D5) and 5-nitrosalicylaldehyde (D6). As the results given in tables, the amino acceptors with aryl group have comparatively good reactivity, and the aryl ketones and aromatic aldehydes presents similar results. However, the low reactivity is observed in the case where the selected aliphatic ketones or aldehydes were used as amino acceptors. In comparison, the reactivity of the ω-TA towards aliphatic ketones and aldehydes was different from previously reported results [41]. It should be noted that in most cases the benzene ring with stronger electron withdrawing group or the methyl with substituent group in aryl ketones

would dramatically inhibit the reactivity of the amino acceptors, and the existence of methylene between aryl group and aldehyde group also significantly reduced the activity of the ω-TA to aryl aldehydes. Additionally, the ω-TA appears to be reactive to two selected cyclic substrates with ketone groups.

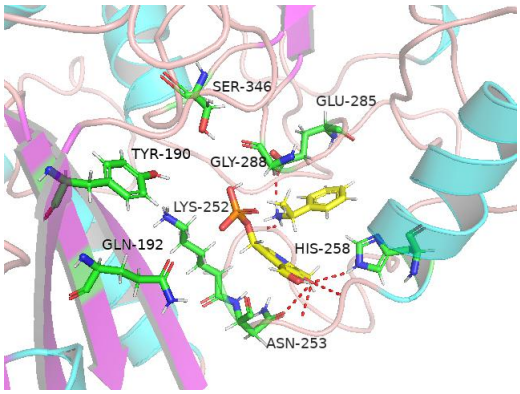

Fig. 5 The model of the active site of the ω-TA binding with PLP and (R)-MBA. The key residues in the active site are shown in green.

Discovery studio proposed an active site model of the ω-TA binding to PLP. The most favorable binding model contains several reported key residues. Previous study has reported that residue K252 shows significant catalytic reactivity with coenzymes and substrates [42]. As is shown in Fig. 5, K252 which binds to the center of the pocket has a strong hydrogen bond force and attractive charge with PLP. At the same time, strong hydrogen bond force was also found between PLP and residues G288 and S346. The residue E285 is located in the substrate-cofactor binding pocket and has conventional hydrogen bonding with the amino group of (R)-MBA. In addition, it is observed that the force contribution of the oxygen atom of phosphate group in PLP was provided by K252, G288 and E285, which is similar to other (R)-selective transaminase [43].

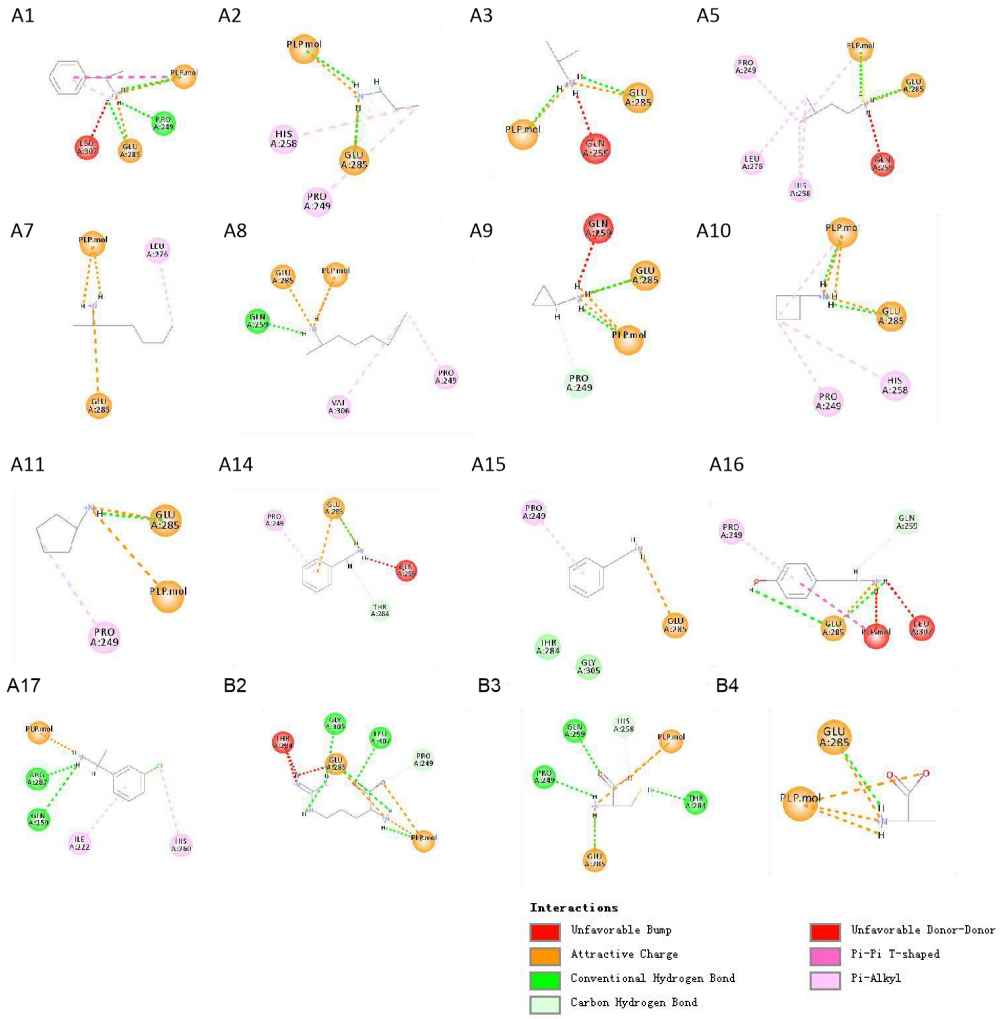

Fig. 6 Docking results of the ω-TA with selected amino donors listed in Table 2 and Table 3

To manage to explain the possible cause of substrate specificity, some selected amino donors and acceptors were docked with ω-TA and PLP, and the results were visualized by Discovery Studio. The most favorable docking configuration was selected to analyze the forces. From the docking results of aliphatic amines (A2-A8), it can be seen that the residues in the binding sphere have Pi-alkyl and attractive charge on the carbon chain, but there is no such force on isopropylamine (A3). Meanwhile, the residue Q259 also has unfavorable bump on A3, which explains the low reactivity of A3. According to the docking results of cyclic amines, PLP has strong acting forces such as Pi-cation interaction and conventional hydrogen bond on the amino groups of cyclic substrates cyclobutanamine (A10) and cyclopentylamine (A11), while the acting force on amino groups of cyclopropylamine (A9) is only C-H bond. This indicates that with the increase of the size of the cyclic substrate, the L-pocket becomes more suitable for binding ligands. When

aromatic substrates were involved, there were many intermolecular forces between the residue in the binding sphere and the benzene ring, including T-shaped Pi-Pi stack and Pi-alkyl interaction. Taking (R)-1-(3-chlorophenyl) ethylamine (A17) as an example. we can see that residues R287 and Q259 have strong conventional hydrogen bond with amino group of A17, and chloro group in benzene ring is an electron-withdrawing group forming Pi-alkyl force with residue H260, which may lead to high reactivity of A17. In addition, the low activity of benzylamine (A14) may be due to the fact that coenzyme PLP has no interaction with it, and residue E259 also has an Unfavorable Donor-Donor to its amino group.

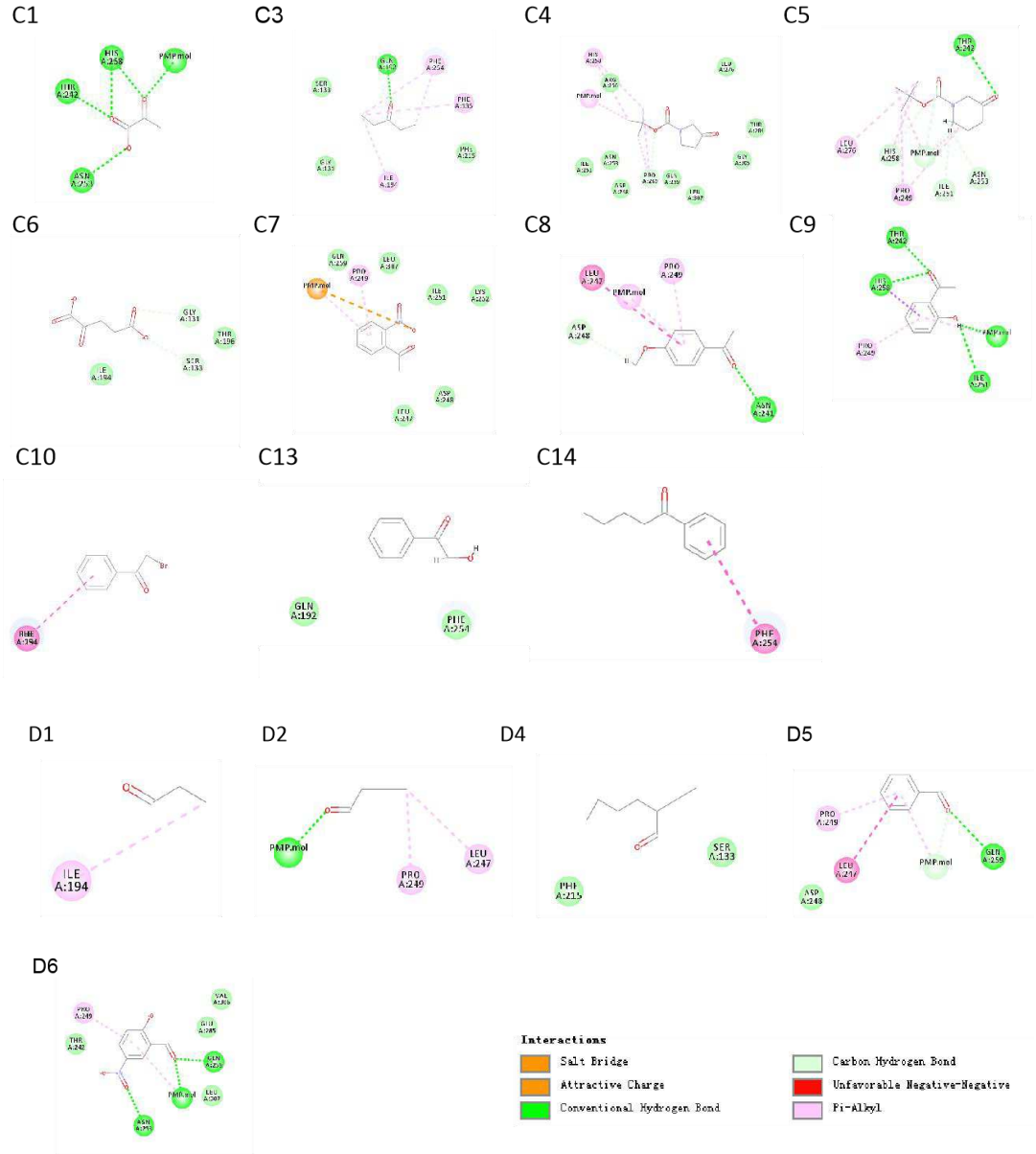

Fig. 7 Docking results of the ω-TA with selected amino acceptors listed in Tables 4 and Table 5

The docking results of the selected amino acceptors with the active site model of the ω-TA binding to PLP. are shown in Fig. 7. We can observed that pyridoxamine 5'-phosphate (PMP) has a strong hydrogen bond to the aldehyde group in the typical acceptor pyruvate (C1), and residues T242, N253, and H258 also bear corresponding hydrogen bond to the aldehyde group and carboxyl group, indicating that the ω-TA has a strong affinity for pyruvic acid. As for α-ketoglutarate (C6), the interaction between PMP and substrate was not found, which may be the reason why the ω-TA has no activity on C6. From the docking results of ketones, it could be perceived that the active site of PMP and the enzyme tended to bind to stable structures containing benzene rings or rings, and only exhibited weak van der waals for straight chain substrates, which might be the reason why most of the aliphatic ketones were low or even inactive, e.g. pentanone (C3). For aromatic ketones, the electron-withdrawing groups of 2'-nitroacetophenone (C7) with good reactivity shows the attractive charge and salt bridge with PMP. In the case of 4'-methoxyacetophenone (C8), PMP has Pi-alkyl interaction to its benzene ring, and residues L242 and N241 have Pi-Pi T-shaped interaction and hydrogen bond to the benzene ring and ketone groups, with its methoxy group having additional C-H interaction binding to the ω-TA. In contrast to other acceptors, the substituted R2 groups show little interaction with the ω-TA and PMP, suggesting that the small pocket of the ω-TA are not suitable for substrates with R2 more than one methyl group, which may be responsible for the lack of activity of 2-hydroxyacetophenone (C13) and valerophenone (C14). For aldehydes, residues in both PMP and the binding sphere have a conventional hydrogen bond to the aldehyde group except for propionaldehyde (D1) and 2-ethylhexanal (D4), which explains the low reactivity of D1 and D4. With regard to the most reactive amino acceptors benzaldehyde (D5) and 5-nitrosalicylaldehyde (D6), residue G259 exerted a strong force on the aldehyde groups of D5 and D6, which was not available for other aldehydes from the docking results. In addition, the nitro group of D6 has an additional conventional hydrogen bond with the active site as an electron withdrawing group.

3.6 Site-saturation mutagenesis of the ω-TA

Enzymatic transamination of ketones to amines is an important method to obtain various chiral building blocks or pharmaceuticals. In this study, a new ω-TA was obtained and its enzymatic properties and substrate spectrum were determined, showing the potential of the ω-TA for the production of chiral amines and unnatural amino acids. However, the unsatisfactory activity on

many ketones of the ω-TA is a vital obstacle for its application in chiral amine production. In order to improve its activity, site-saturation mutagenesis was conducted on the basis of previous results and homology modeling.

As confirmed by Voss et al, residues F130, Y190, Q190, G288, and A348 showed significant influence on the activity of amine transaminase. Docking result of the ω-TA with PLP and (R)-MBA indicated that residues K252, E285, G288, Q192 and Y190 are all located in the small pocket of the active site. Hereby, residues Y190, Q192, and G288 were selected for site saturation mutation, and the results are presented in Fig. 9. The results showed that the changes in residues Y190 and Q192 did have a significant effect on the activity of the ω-TA to (R)-MBA. Among them, mutant Q192G was the most beneficial mutation (Fig. 10). However, there was no significant change in the activity of mutants G288 for the ω-TA. The ω-TA and mutant Q192G was used to convert acetophenone to produce (R)-MBA, and results showed that after 16 h of reaction, the conversion of (R)-MBA for mutant Q192G was around 55% with e.e. ≥99%, which was more than seven times higher than that of the ω-TA.

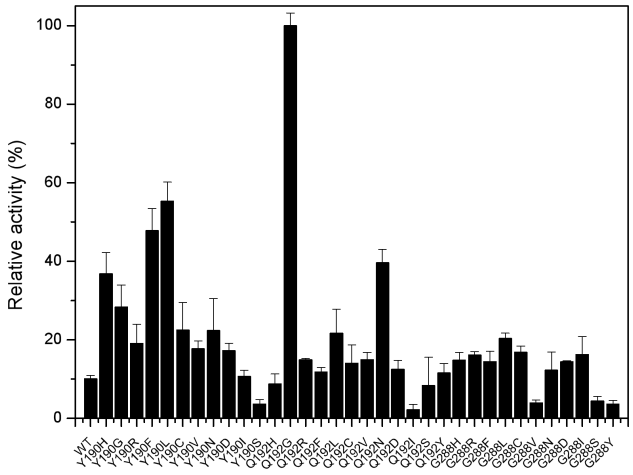

Fig. 9 The results of site saturation mutation of the ω-TA.

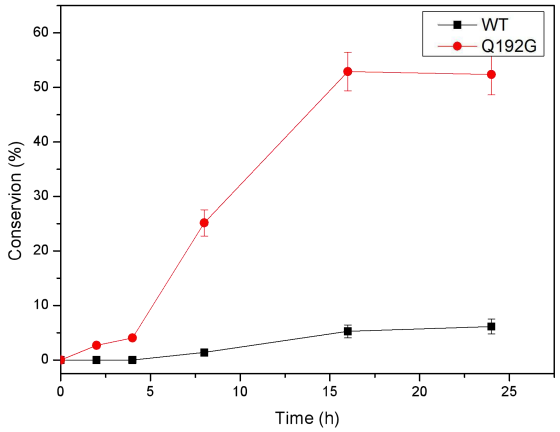

Fig. 10 The conversion of (R)-MBA by the ω-TA and mutant Q192G. 0.1 mg mL^{-1} purified enzyme, 25 mM D-alanine (D-Ala), 25 mM acetophenone, 0.02 mM PLP, 1 mL glycine-NaOH buffer (50 mM, pH 8.5), and 45 °C.

Subsequently, the ω-TA and mutant Q192G were further applied to evaluate the conversion of cyclic substrates with ketone group, and results are shown in Fig. 10. After 36 h of reaction, the conversion of *N*-Boc-pyrrolidinone and *N*-Boc-piperidone by the ω-TA was about 15% and 12%, and the conversion of *N*-Boc-pyrrolidinone and *N*-Boc-piperidone by mutant Q192G was increased to 23% and 30%, respectively. Compared with the ω-TA, the activity of mutant Q192G was improved evidently. However, further study is necessary to continually enhance the activity of the ω-TA.

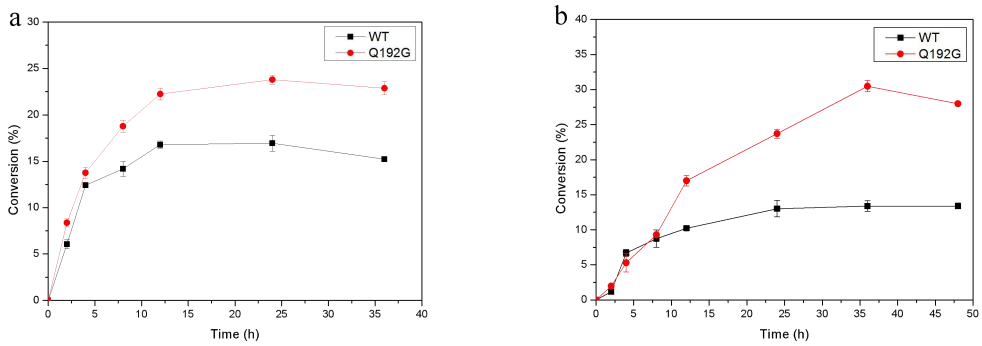

Fig. 11 Conversion of *N*-Boc-3-pyrrolidinone and *N*-Boc-3-aminopiperidine by the ω-TA and its Q192G mutant: **a)** *N*-Boc-3-pyrrolidinone; **b)** *N*-Boc-3-aminopiperidine. Reaction conditions: 0.1 mg mL^{-1} purified enzyme, 25 mM D-Ala, either 25 mM *N*-Boc-pyrrolidinone or *N*-Boc-piperidone, 0.02 mM PLP, 1 mL glycine-NaOH buffer (50 mM, pH 8.5), and 45 °C.

4 Conclusion

(R)–Selective ω-TAs has important potential for industrial applications. In this work, a hypothetical (R)- selective ω-TA from *C. bacterium* was found by motif sequence blast from genome mining. On the basis of the amino acid sequences, a phylogenetic tree was constructed to verify the taxonomic and evolutionary relationships of the ω-TA with other amine transaminase family homologues. Ten amino acid sequences with different degrees of sequence identity to the ω-TA were selected and analyzed, and the ω-TA showed a close evolutionary relationship to pyruvate transferase from *M. vanbaalenii* PYR-1 and Ata-117 Arrmut11. By characterizing the enzymatic properties of the recombinant ω-TA, results showed that the ω-TA has good thermal stability, organic solvent tolerance and broad substrate specificity. Thereafter, the site-saturation mutation of the ω-TA was conducted and the mutant Q192G with higher activity was screened, which was applied in a conversion of *N*-Boc-pyrrolidinone and *N*-Boc-piperidone. Results showed that the ω-TA can be used as a valuable catalyst for the asymmetric synthesis of chiral amines from the corresponding aldehydes or ketones.

Abbreviations

PLP :Pyridoxal 5'-phosphate

PMP :Pyridoxamine 5'-phosphate

D-Ala :D-alanine

(R)-MBA :(R)-methylbenzylamine

ω-TA :ω-transaminase

HPLC :High Performance Liquid Chromatography

IPTG :Isopropyl β-D-1-thiogalactopyranoside

PCR : Polymerase Chain Reaction

SDS-PAGE :Sodium dodecyl sulfate polyacrylamide gel electrophoresis

ee :Enantiomeric excess

Availability of data and materials

The data and the materials are all available in this article.

Acknowledgements

We acknowledged the financial support from Jiangsu Agricultural Science and Technology Innovation Fund Project (CX(19)2001), Qing Lan Project of Jiangsu Universities, and Six Talent Peaks Project in Jiangsu Province, the Jiangsu Synergetic Innovation Center for Advanced Bio-manufacture, and PAPD.

Funding

Jiangsu Agricultural Science and Technology Innovation Fund Project (CX(19)2001), Qing Lan Project of Jiangsu Universities, and Six Talent Peaks Project in Jiangsu Province, the Jiangsu Synergetic Innovation Center for Advanced Bio-manufacture, and PAPD.

Author information

Affiliations

College of Biotechnology and Pharmaceutical Engineering, Nanjing Tech University,

Nanjing 211800, China

Chen Wang, Kexin Tang, Ya Dai, Honghua Jia, Yan Li, Zhen Gao & Bin Wu

Contributions

C.W. conducted most of the experiments. Y.L. and H.H.J. designed and supervised the project. All the authors discussed the design and results, commented on the manuscript, and approved the manuscript.

Ethics declarations

Ethics approval and consent to participate

Not applicable.

Consent for publication

Not applicable.

Competing interests

The authors declare no conflict of interest.

References

1. Rehn G, Adlercreutz P, Grey C (2014) Supported liquid membrane as a novel tool for driving the equilibrium of ω-transaminase catalyzed asymmetric synthesis. J Biotechnol 179: 50–55. doi：10.1016/j.jbiot ec.2014.03.022.

2. Fuchs M, Farnberger JE, Kroutil W (2015) The industrial age of biocatalytic transamination. Eur J Org Chem 32: 6965–6982. doi:10.1002/ejoc.201500852.

3. Höhne M, Bornscheuer UT (2009) Biocatalytic routes to optically active amines. Chemcatchem 1: 42–51. doi:10.1002/cctc.200900110.

4. Kroutil W, Fischereder EM, Fuchs CS, Lechner H, Mutti FG, Pressnitz D,Rajagopalan A, Sattler JH, Simon RC, Siirola E (2013) Asymmetric preparation of prim-, sec-, and tert-amines employing selected biocatalysts. Org Process Res Dev 17: 751–759. doi:10.1021/op4000237.

5. Kohls H, Steffen-Munsberg F, Höhne M (2014) Recent achievements in developing the biocatalytic toolbox for chiral amine synthesis. Curr Opin Chem Biol 19: 180–192. doi:10.1016/j.cbpa.2014.02.021.

6. Fuchs M, Farnberger E, Kroutil W (2015) The industrial age of biocatalytic transamination. Eur J Org Chem 32: 6965–6982. doi:10.1002/ejoc.20150 0852.

7. Guo F, Berglund P (2017) Transaminase biocatalysis: optimization and application. Green Chem 19: 333–360. doi:10.1039/C6GC0 2328B.

8. Kara S, Schrittwieser JH, Hollmann F, Ansorge-Schumacher MB (2014) Recent trends and novel concepts in cofactor-dependent biotransformations. Appl Microbiol Biotechnol 98: 1517–1529. doi:1517.10.1007/s00253-013-5441-5.

9. Koszelewski D, Tauber K, Faber K, Kroutil W (2010) ω-Transaminases for the synthesis of non-racemic α-chiral primary amines. Trends Biotechnol 28: 324–332. doi:10.1016/j.tibtech.2010.03.003.

10. Savile CK, Janey JM, Mundorf EC, Moore JC, Tam S (2010) Biocatalytic asymmetric synthesis of chiral amines from ketones applied to sitagliptin manufacture. Science 329: 305–309. doi: 10.1126/science.1188934

11. Park ES, Kim M, Shin JS (2012) Molecular determinants for substrate selectivity of ω-transaminases. Appl Microbiol Biotechnol 93: 2425–2435. doi:10.1007/s00253-011-3584-9.

12. Malik MS, Park ES, Shin JS (2012) Features and technical applications of ω-transaminases. Appl Microbiol Biotechnol 94: 1163–1171. doi:10.1007/s00253-012-4103-3.

13. Höhne M, Bornscheuer UT (2009) Biocatalytic routes to optically active amines. ChemCatChem 1: 42–51. doi:10.1002/chin.200946255

14. Höhne M, Schatzle S, Jochens H, Robins K, Bornscheuer UT (2010) Rational assignment of key motifs for function guides in silico enzyme identification. Nat Chem Biol 6: 807–813. doi:10.1038/nchembio.447.

15. Jiang JJ, Chen X, Zhang DL, Wu QQ, Zhu DM (2014) Characterization of (R)-selective amine transaminases identified by in silico motif sequence blast. Appl Microbiol Biotechnol 99: 2613–2621. doi:10.1007/s00253-014-6056-1.

16. Zeifman YS, Boyko KM, Nikolaeva AY, Timofeev VI, Rakitina TV, Popov VO, Bezsudnova EY (2019) Functional characterization of PLP fold type IV transaminase with a mixed type of activity from *Haliangium ochraceum*. BBA-Proteins Proteom 1867: 575–585. doi:10.1016/j.bbapap.2019.03.005.

17. Bezsudnova EY, Dibrova DV, Nikolaeva AY, Rakitina TV, Popov VO (2018) Identification of branched-chain amino acid aminotransferases active towards (R)-(+)-1-phenylethylamine among PLP fold type IV transaminases. J Biotechnol 271:26–28. doi:10.1038/s41598-017-15520-4.

18. Skalden L, Thomsen M, Hohne M, Bornscheuer UT, Hinrichs W (2015) Structural and biochemical characterization of the dual substrate recognition of the (R)-selective amine transaminase from *Aspergillus fumigates*. FEBS J 282: 407–415. doi:10.1111/febs.13149.

19. Voss M, Xiang C, Esque J, Nobili A, Menke MJ, André I, Höhne M, Bornscheuer UT (2020) Creation of (R)-amine transaminase activity within an α-amino acid transaminase scaffold. ACS

Chem Biol 15: 416–424. doi:10.1021/acschembio.9b00888..

20. Cheng F, Chen XL, Xiang C, Liu ZQ, Wang YJ, Zheng YG (2020) Fluorescence-based high-throughput screening system for R-omega-transaminase engineering and its substrate scope extension. Appl Microbiol Biotechnol 104: 2999–3009. doi:10.1007/s00253-020-10444-y.

21. Cheng F, Chen XL, Li MY, Zhang XJ, Jia DX, Wang YJ, Liu ZQ, Zheng YG (2020) Creation of a robust and R-selective omega-amine transaminase for the asymmetric synthesis of sitagliptin intermediate on a kilogram scale. Enzyme Microb Technol 141: 109655. doi:10.1016/j.enzmictec.2020.109655.

22. Sudhir K, Glen S, Koichiro T (2016) MEGA7: Molecular evolutionary genetics analysis version 7.0 for bigger datasets. Mol Biol Evol 33: 1870–1874. doi:10.1093/molbev/msw054.

23. Saitou N, Nei M, (1987) The neighbor-joining method: a new method for reconstructing phylogenetic trees. Mol Biol Evol 4: 406–425. doi:10.1093/oxfordjournals.molbev.a040454.

24. Schägger H, Jagow GV (1987) Tricine-sodium dodecyl sulfate-polyacrylamide gel electrophoresis for the separation of proteins in the range from 1 to 100 kDa. Anal Biochem 166 : 368–379. doi:10.1016/0003-2697(87)90587-2.

25. Shin JS, Kim BG (2002) Exploring the active site of amine: pyruvate aminotransferase on the basis of the substrate structure-reactivity relationship: how the enzyme controls substrate specificity and stereoselectivity. J Org Chem 67: 2848–2853. doi:10.1021/jo016115i.

26. Petri A, Colonna V, Piccolo O (2019) Asymmetric synthesis of a high added value chiral amine using immobilized ω-transaminases. Beilstein J Org Chem 15: 60–66. doi:10.3762/bjoc.15.6.

27. Shin JS, Kim BG (2001) Comparison of the omega-transaminases from different microorganisms and application to production of chiral amines. Biosci Biotechnol Biochem 65: 1782–1788. https://doi.org/10.1271/bbb.65.1782.

28. Steffen-Munsberg F, Vickers C, Thontowi A, Schätzle S, Meinhardt T (2013) Revealing the structural basis of promiscuous amine transaminase activity. ChemCatChem 5: 154–157. doi:10.1002/cctc.201200545.

29. Iwasaki A, Matsumoto K, Hasegawa J, Yasohara Y (2012) A novel transaminase, (R)-amine: pyruvate aminotransferase, from *Arthrobacter* sp. KNK168 (FERM BP-5228): purification, characterization, and gene cloning. Appl Microbiol Biotechnol 93: 1563–1573. doi:

10.1007/s00253-011-3580-0.

30. Boyko KM, Stekhanova TN, Nikolaeva AY, Mardanov AV, Ravin NV, Bezsudnova EY, Popov VO (2016) First structure of archaeal branched-chain amino acid aminotransferase from *Thermoproteus uzoniensis* specific for L-amino acids and R-amines. Extremophiles 20: 215–225. doi: 10.1007/s00792-016-0816-z.

31. Chen YJ, Yi D, Jiang SQ, Wei DZ (2016) Identification of novel thermostable taurine–pyruvate transaminase from *Geobacillus thermodenitrificans* for chiral amine synthesis. Appl Microbiol Biotechnol 100: 3101–3111. doi:10.1007/s00253-015-7129-5.

32. Bruins ME, Boom JRM (2001) Thermozymes and their applications. Appl Biochem Biotechnol 90: 155–186. doi:10.1385/ABAB:90:2:155.

33. Atalah J, Cáceres-Moreno, P, Espina G, Blamey JM (2019) Thermophiles and the applications of their enzymes as new biocatalysts. Bioresour Technol 280, 478–488. doi:10.1016/j.biortech.2019.02.008.

34. Mathew S, Deepankumar K, Shin G, Hong EY, Kim BG, Chung T, Yun H (2016) Identifification of novel thermostable ω-transaminase and its application for enzymatic synthesis of chiral amines at high temperature. RSC Adv 6: 69257–69260. doi:10.1039/C6RA15110H.

35. Ferrandi EE, Bassanini I, Sechi B, Vanoni M, Tessaro D, Guðbergsdóttir SR, Riva S, Peng X, Monti D (2020) Discovery and characterization of a novel thermostable β-amino acid transaminase from a *Meiothermus* strain isolated in an icelandic hot spring. Biotechnol J 15: 2000125. doi:10.1002/biot.202000125.

36. Ferrandi EE, Previdi A, Bassanini I, Riva S, Monti D (2017) Novel thermostable amine transferases from hot spring metagenomes. Appl Microbiol Biotechnol 101: 1–17. doi:10.1007/s00253-017-8228-2.

37. Kelly SA, Magill DJ, Megaw J, Skvortsov T, Mcgrath JW, Allen CCR, Moody TS (2019) Characterisation of a solvent-tolerant haloarchaeal (R)-selective transaminase isolated from a Triassic Period salt mine. Appl Microbiol Biotechnol 103: 5727–5737. doi:10.1007/s00253-019-09806-y.

38. Gao SH, Su Y, Zhao L, Li GD, Zheng GJ (2017) Characterization of a (R)-selective amine transaminase from *Fusarium oxysporum*. Process Biochem 63: 130–136. doi:10.1016/j.procbio.2017.08.012.

39. Pavlidis IV, Wei MS, Genz M, Spurr P, Hanlon SP, Wirz B, Iding H, Bornscheuer UT (2016) Identiication of (S)-selective transaminases for the asymmetric synthesis of bulky chiral amines. Nat Chem 8: 1076–1082. doi:10.1038/nchem.2578

40. Iglesias C, Panizza P, Giordano RS (2017) Identification, expression and characterization of an R-ω-transaminase from *Capronia semiimmersa*. Appl Microbiol Biotechnol 101: 5677–5687. doi:10.1007/s00253-017-8309-2

41. Jiang J, Chen X, Feng J, Wu Q, Zhu D (2014) Substrate proile of an ω-transaminase from *Burkholderia vietnamiensis* and its potential for the production of optically pure amines and unnatural amino acids. J Mol Catal B 100: 32–39. doi:10.1016/j.molca tb.20131.013.

42. Eliot AC, Kirsch JF (2004) Pyridoxal phosphate enzymes: mechanistic, structural, and evolutionary considerations. Annu Rev Biochem 73: 383–415. doi:10.1146/annurev.biochem.73.01130 3.074021.

43. Skalden L, Thomsen M, Höhne M, Bornscheuer UT, Hinrichs W (2014) Structural and biochemical characterization of the dual substrate recognition of the (R)-selective amine transaminase from *Aspergillus fumigatus*. FEBS J 282: 407–415 doi:10.1111/febs.13149.

Figures

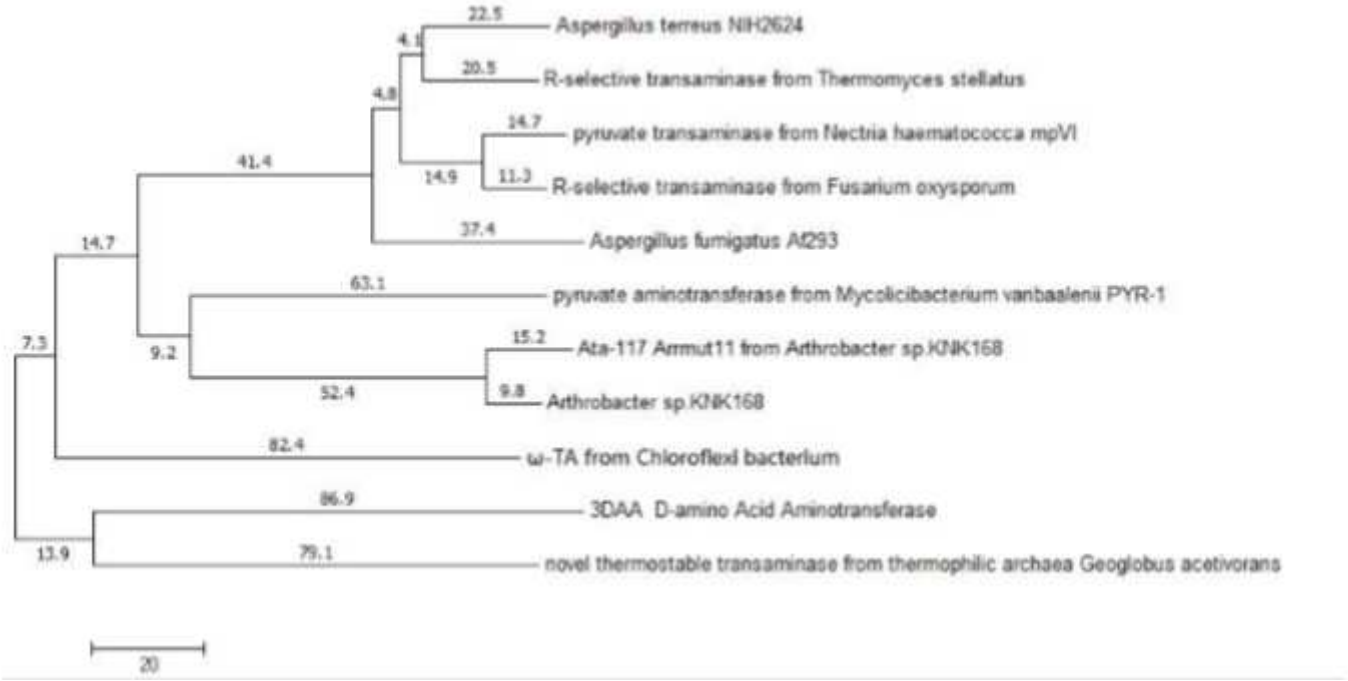

Figure 1

Phylogenetic analysis of the ω-TA from C. bacterium and related proteins. The phylogenetic tree was constructed using the neighbor-joining algorithm in the molecular evolutionary genetics analysis package (MEGA 7) and highlighted the relative positions of the proteins labeled with the species names.

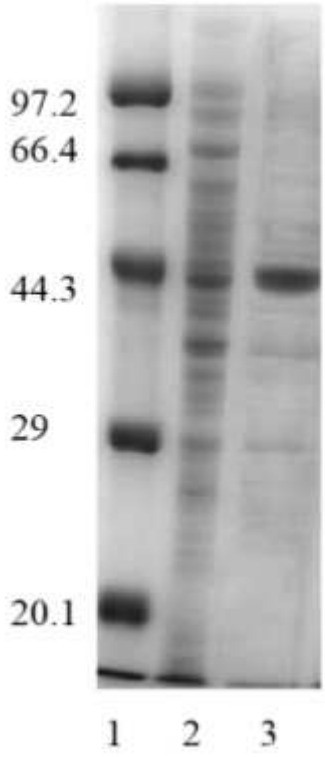

Figure 2

SDS-PAGE of the ω-TA. Lane 1, protein markers; Lane 2, crude extract; Lane 3, purified enzyme

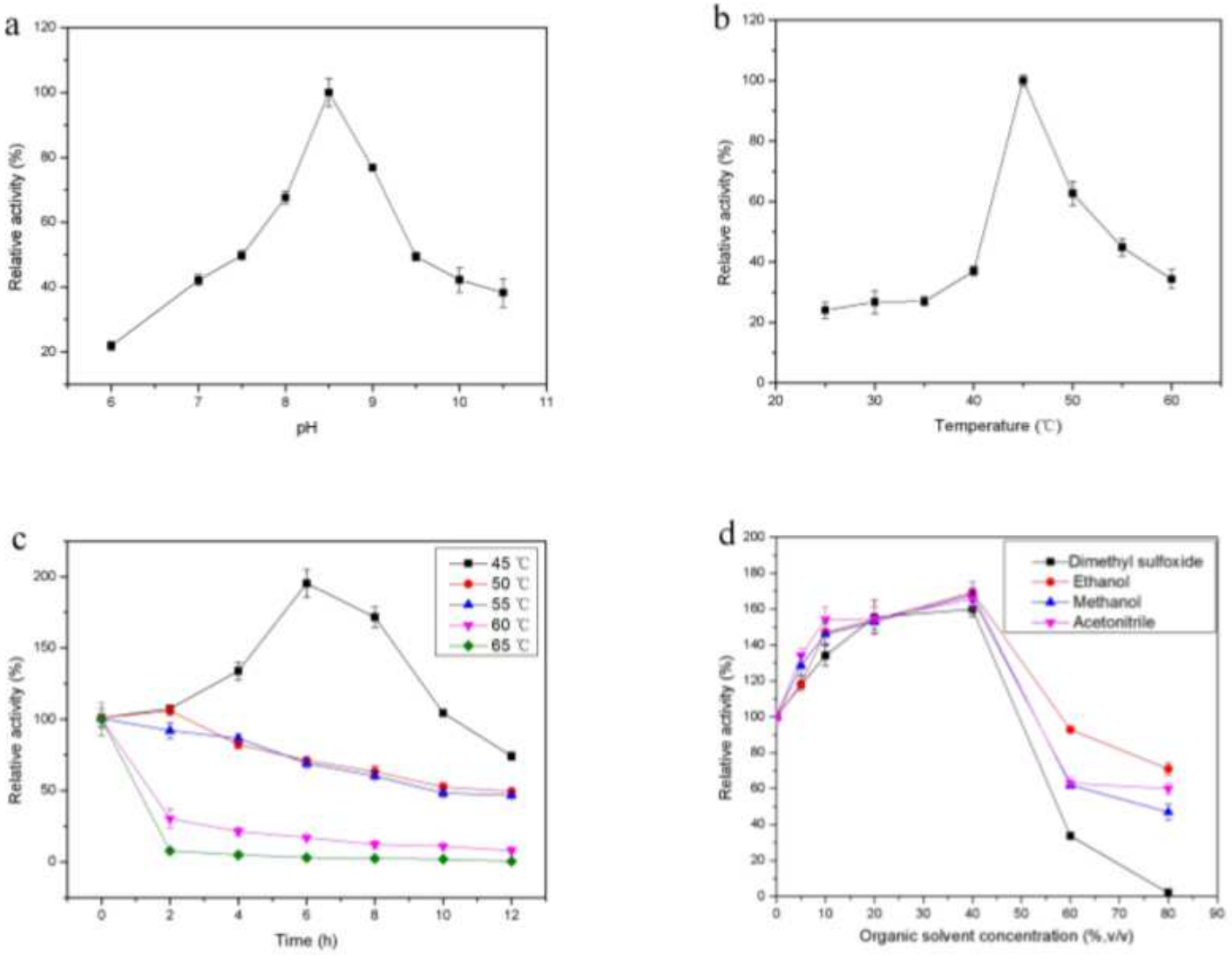

Figure 3

Characterization of enzymatic properties of the ω-TA. a) Optimum pH; b) Optimum temperature; c) Temperature stability; d) Effect of Organic cosolvent concentration on the ω-TA activity.

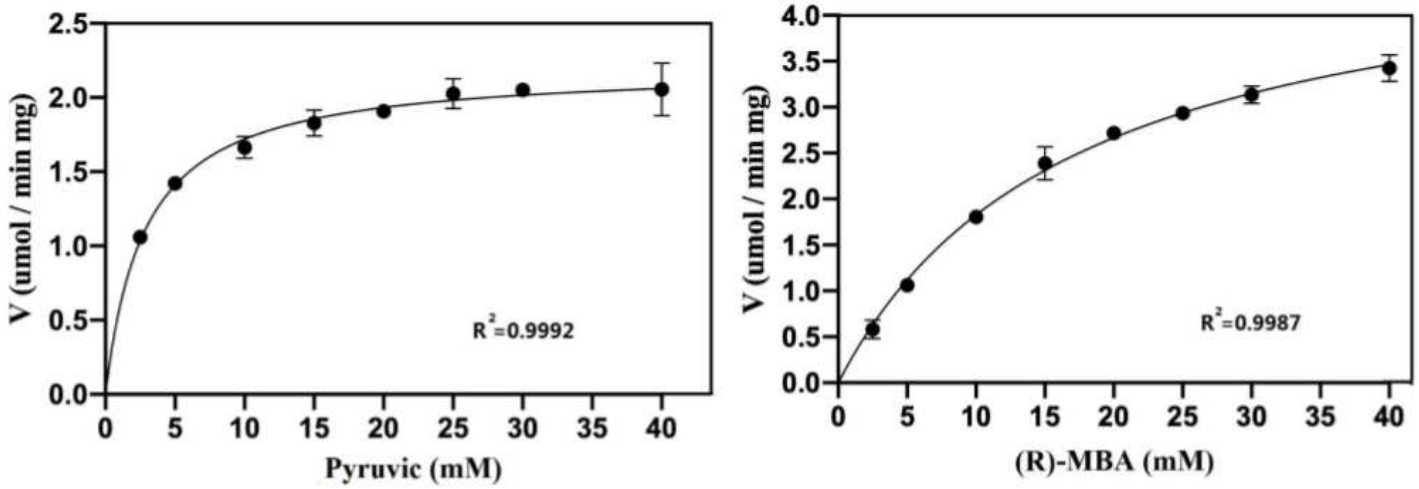

Figure 4

The nonlinear regression fitting of Michaelis-Menten equation

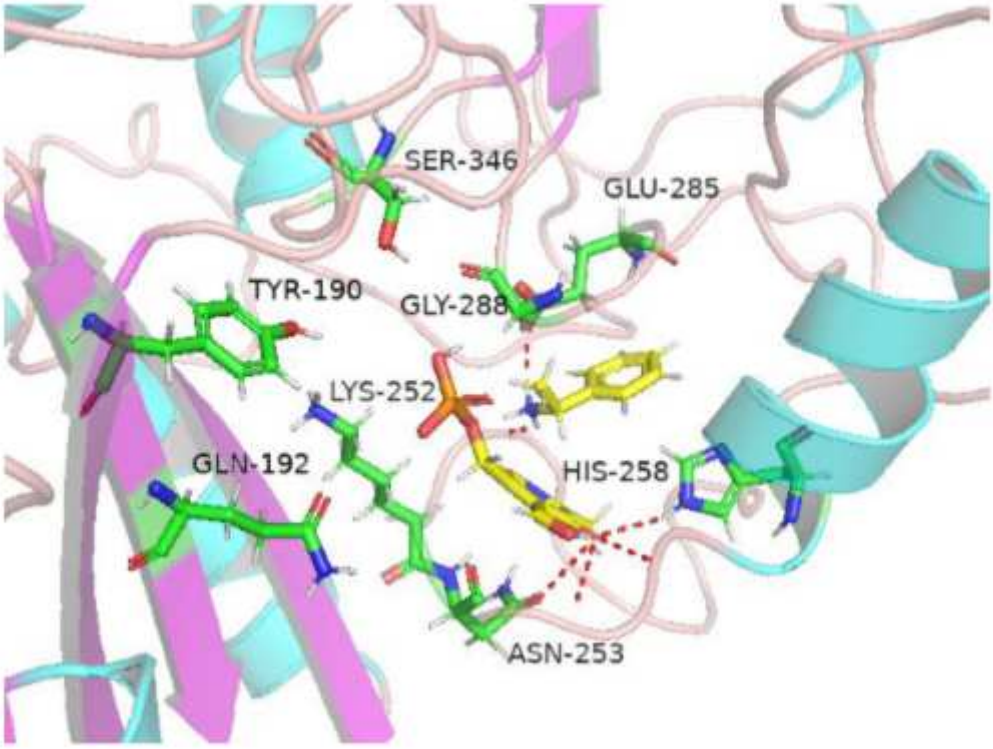

Figure 5

The model of the active site of the ω-TA binding with PLP and (R)-MBA. The key residues in the active site are shown in green.

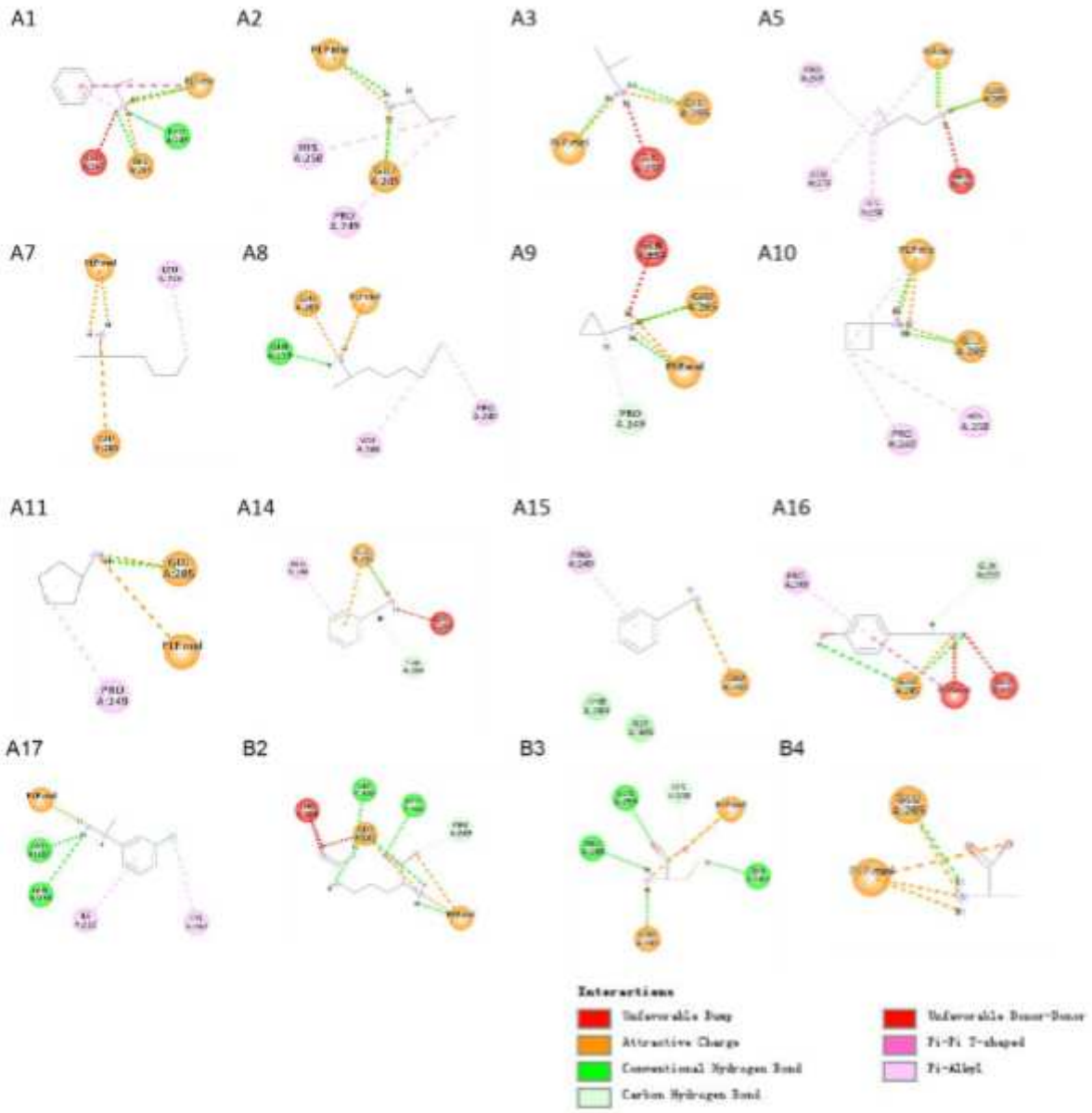

Figure 6

Docking results of the ω-TA with selected amino donors listed in Table 2 and Table 3

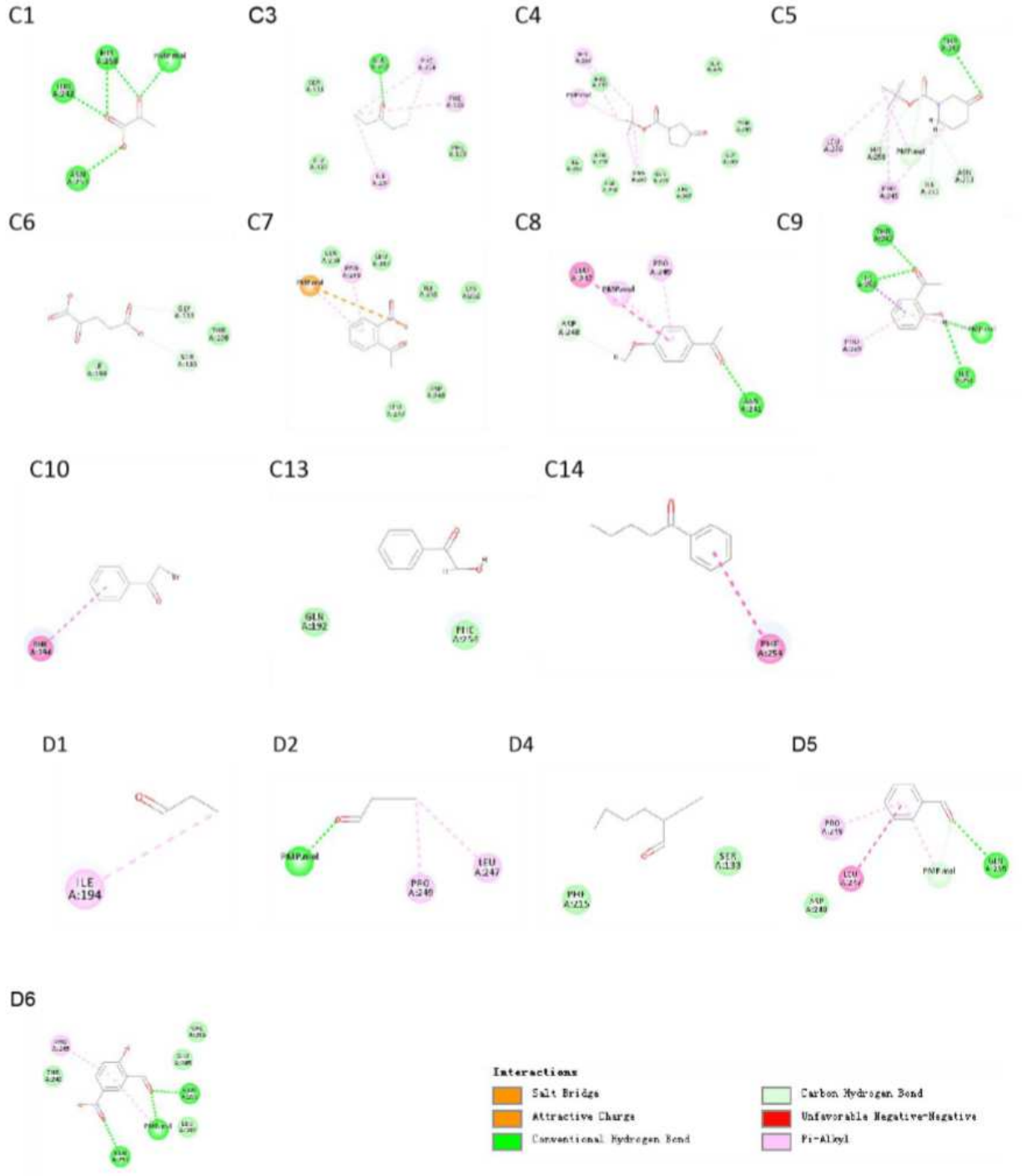

Figure 7

Docking results of the ω-TA with selected amino acceptors listed in Tables 4 and Table 5

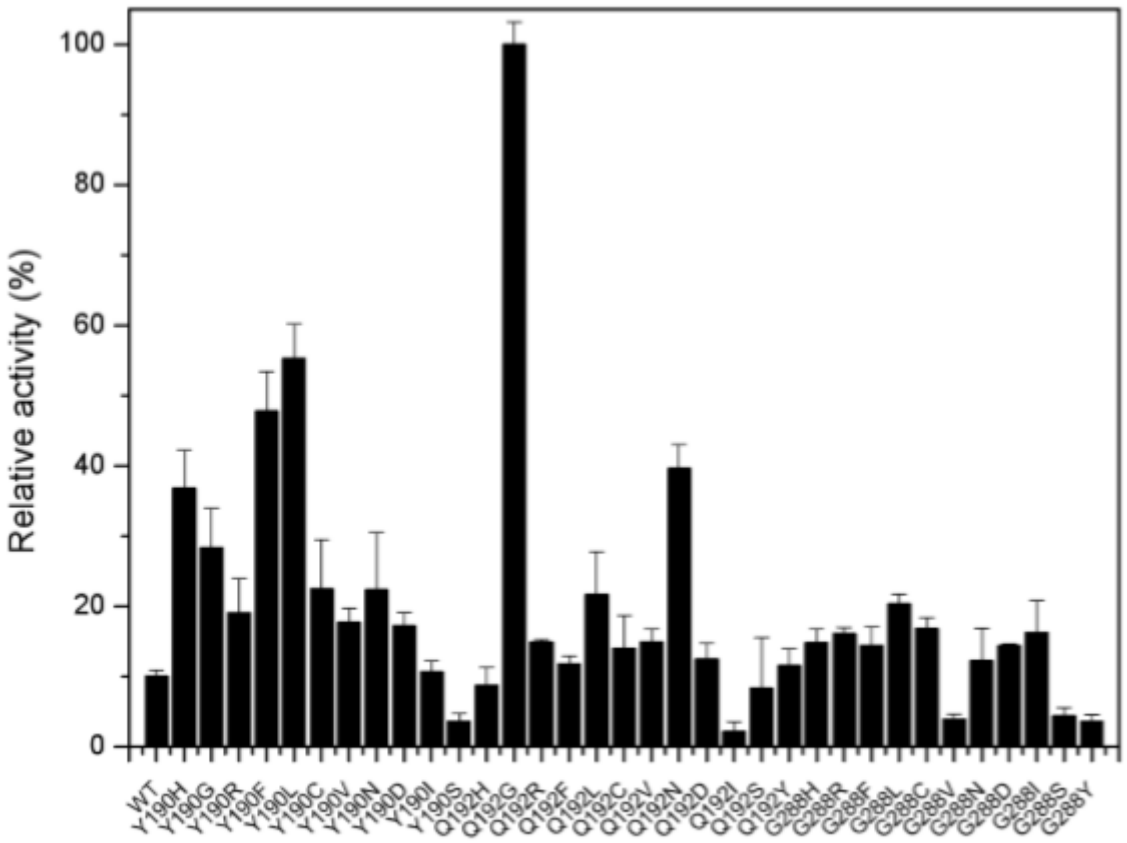

Figure 8

The results of site saturation mutation of the ω-TA.

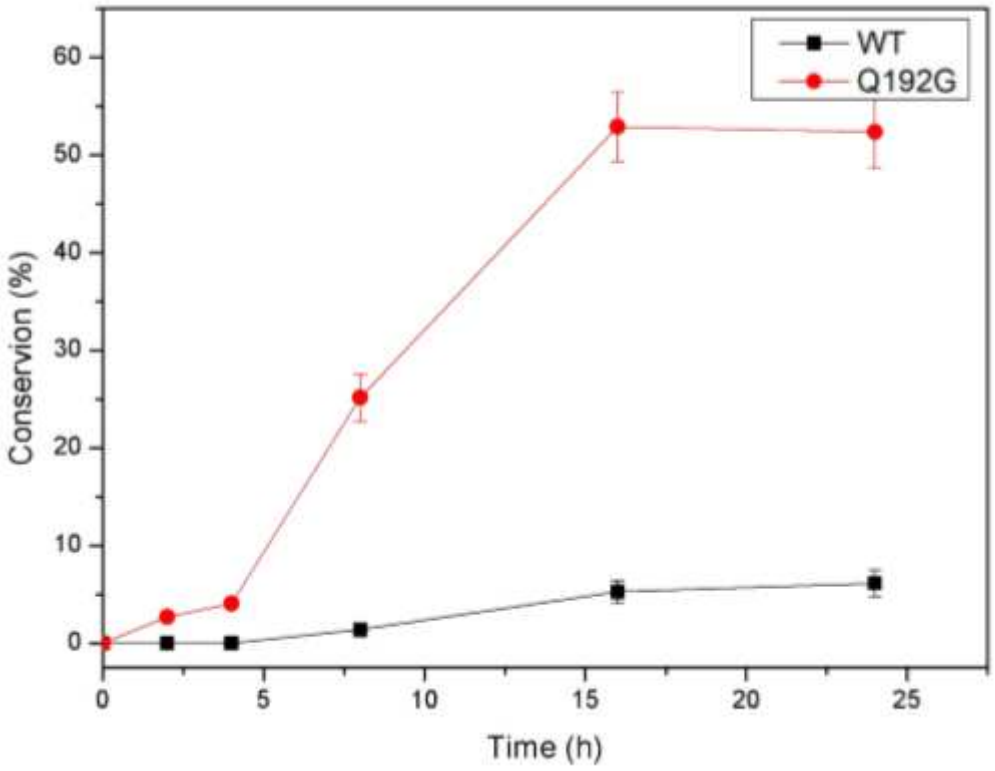

Figure 9

The conversion of(R)-MBA by theω-TA and mutant Q192G.0.1 mg mL−1 purified enzyme ,25mM D-alanine(D-Ala), 25 mM acetophenone, 0.02 mM PLP, 1mL glycine-NaOH buffer (50mM, pH8.5),and 45°C.

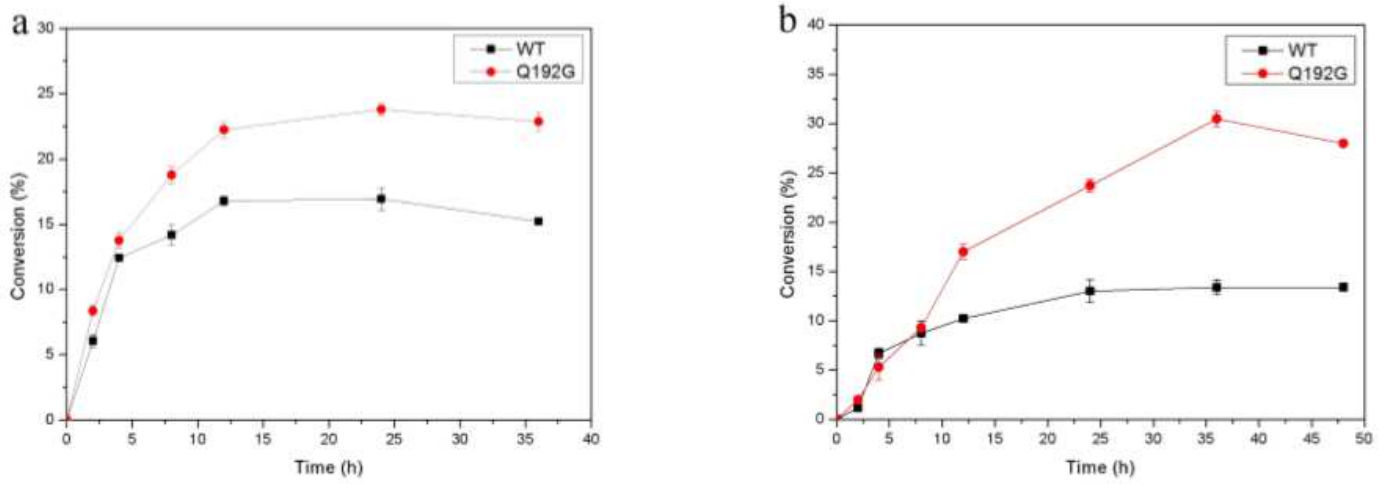

Figure 10

Conversion of N-Boc-3-pyrrolidinoneand N-Boc-3-aminopiperidine by the ω-TA and its Q192G mutant: a) N-Boc-3-pyrrolidinone; b)N-Boc-3-aminopiperidine. Reaction conditions: 0.1mgmL−1 purified enzyme, 25mM D-Ala, either 25mM N-Boc-pyrrolidinone or N-Boc-piperidone, 0.02mM PLP, 1mL glycine-NaOH buffer(50mM, pH8.5), and 45°C.

Supplementary Files

This is a list of supplementary files associated with this preprint. Click to download.

- abstract.png